ELSEVIER

Journal of Electroanalytical Chemistry 523 (2002) 16–25

Journal of Electroanalytical Chemistry

www.elsevier.com/locate/jelechem

Stripping chronopotentiometry for metal ion speciation analysis at a microelectrode

Herman P. van Leeuwen [a], Raewyn M. Town [b,*]

[a] *Laboratory of Physical Chemistry and Colloid Science, Wageningen University, Postbus 8038, Dreijenplein 6, 6703 HB Wageningen, Netherlands*

[b] *School of Chemistry, The Queen's University of Belfast, David Keir Building, Belfast BT9 5AG, Northern Ireland, UK*

Received 3 December 2001; received in revised form 30 January 2002; accepted 31 January 2002

Abstract

The features of metal ion speciation determination by stripping chronopotentiometry (SCP) at a microelectrode are examined and compared with those of DP-SV. SCP measurements are essentially of a steady-state nature under experimentally achievable conditions and correspond to practically complete depletion of the microelectrode. SCP data for simple systems (pyridine-2,6-dicarboxylate complexes with Cd(II) and Pb(II)) and a heterogeneous system (Pb(II)–fulvic acid) were in general agreement with the recently developed theory that predicts reduced lability at microelectrodes due to enhanced diffusion. Furthermore, SCP measurements were not influenced by adsorption processes nor by the ligand-to-metal ratio at the electrode surface during stripping. In contrast, DP-SV data could not be interpreted in a straightforward manner due to (i) adsorption-induced enhancement of the stripping signals and (ii) severe peak distortion arising from saturation of the ligand at the electrode surface during stripping.

Keywords: Microelectrode; Lability; Metal speciation; Stripping chronopotentiometry; Voltammetry

1. Introduction

Electrochemical techniques, especially stripping methods, are of particular relevance for studies on metal ion speciation. They provide adequate sensitivity and the analytical signals inherently contain direct speciation information. In particular, electrochemical methods are sensitive to the stability, rates of association and dissociation (manifested in the measured lability, that is governed by the effective time scale of the technique), and size (diffusion coefficient) of metal complex species. The speciation sensitive step is the deposition (preconcentration) step, during which metal ions are reduced at a constant potential for a fixed time and accumulate in the working electrode (usually mercury). The accumulated metal is quantified by a stripping (oxidation) step: in stripping voltammetry (SV) an anodically ramping voltage is applied and the resulting current is recorded as a function of potential; in stripping chronopotentiometry (SCP) quantification is achieved by application of a constant oxidising current (or by flux of a chemical oxidant) and the analytical signal is the potential as a function of time (the time taken for reoxidation, or transition time, τ_{tr}, is proportional to the amount of metal accumulated).

The significance of dynamic aspects of speciation for understanding the reactivity and bioavailability of metal complex species is becoming increasingly realised [1–5]. In environmental and biological media, the speciation of trace metals is often controlled by heterogeneous macromolecular ligands such as humic substances [6]. Interpretation of stripping voltammetric data for samples containing heterogeneous ligands with distributed stabilities and labilities is not straightforward, but theoretical frameworks are available [7–10]. Ideally, any determination of metal ion speciation should be made in situ to minimise perturbation of the original equilibria. Measurements in low ionic strength samples, e.g. freshwaters, or measurements to obtain information on spatial resolution, require use of a

* Corresponding author. Tel.: +44-28-9027-4415; fax: +44-28-9038-2117.

E-mail address: r.town@qub.ac.uk (R.M. Town).

0022-0728/02/$ - see front matter
PII: S0022-0728(02)00723-4

microelectrode. Microelectrodes are finding increasing application in in situ measurements of trace metals [11] and there is a plethora of empirical reports on the use of microelectrodes to determine ''labile'' metal in various environmental or biological media [12–16].

To date, however, there has been no rigorous experimental evaluation of the actual metal ion speciation determined by microelectrodes. This aspect is addressed in the present work. Rational interpretation of such measurements in terms of metal speciation requires a sound theoretical understanding of processes occurring at the microsurface. The transition from a macro- to a microelectrode influences the nature and magnitude of the flux to the surface as well as the extent of lability of metal complex species. In practice, the diffusional transport can be considered to be essentially steady-state. This aspect is also of significance for metal bioavailability to microorganisms [17], which highlights the potential utility of microelectrodes for monitoring bioavailable metal species. A theoretical framework for the interpretation of speciation measurements at a microelectrode has recently been developed [18,19].

In this work, we examine the features of SCP measurements of metal ion speciation at a microelectrode and compare them with the more widely used DP-SV. Results from our previous work with a conventional HMDE showed that SCP in the complete depletion regime has comparable sensitivity to DP-SV [20] and is not influenced by adsorption processes [21]. Disproportional current enhancements are known to occur with transient techniques in the presence of product and/or reactant adsorption [22]. To explore the features of SCP and DP-SV at a microelectrode fully we have measured a range of metal complex systems. The simple Pb(II)-pyridine-2,6-dicarboxylic acid (PDCA) and Cd(II)–PDCA systems, due to the stability of their complexes, are expected to have reduced lability at a microelectrode. No adsorption effects occur in the Cd(II)–PDCA system, while in the Pb(II)–PDCA system, adsorption of ML causes peak enhancement of DP-SV signals at a macroelectrode [21]. We have also studied a heterogeneous system (Pb(II)–fulvic acid (FA)) that is representative of metal complex species present in natural waters. This system is labile under our conditions, but the complex has a lower diffusion coefficient than the free metal, and adsorption of both the free ligand and metal complexes will occur.

2. Experimental

2.1. Apparatus

An Ecochemie Autolab PGSTAT10 potentiostat was used; the electrometer input impedance of this instrument is > 100 GΩ. The working electrode was a mercury-coated iridium disk microelectrode (described below), the auxiliary electrode was glassy carbon, and the reference electrode was Ag | AgCl | KCl(sat) encased in a 0.1 mol dm^{-3} KNO_3 jacket. Measurements were performed at 20 °C.

2.2. Working electrode

2.2.1. Preparation of the electrode surface

The working electrode consisted of a hemispherical mercury droplet electrodeposited onto an iridium disk microelectrode (Idronaut, Italy). The iridium surface was initially prepared by successively wet grinding with silicon carbide paper Grit #2400 (10×10^{-6} m; Struers, PAPER 40400117) then Grit #4000 (5×10^{-6} m; Struers, PAPER 40400116), followed by final polishing with 1×10^{-6} m diamond paste (Struers, KITON) on a DP-Mol polishing cloth (Struers, DEKOL) lubricated with DP-Lubricant Blue (Struers, DEPT1). All polishing steps were performed using an automated polishing system (manufactured by the University of Geneva, see Ref. [23] for details). Following this initial preparation of the electrode surface, extensive regular polishing was not required; the surface was maintained by occasional polishing with the 1 μm diamond paste on the polishing cloth.

2.2.2. Characterisation of electrode dimensions

The radius of the bare iridium disc was determined to be 4 μm from the limiting CV current for a solution of 10^{-3} mol dm^{-3} $Ru(NH_3)_6Cl_3$ in phosphate buffer at pH 7.4 (for a disc, $I_l = 4nFDcr$, where $D = 5.3 \times 10^{-10}$ m^2 s^{-1} [24]). The hemispherical mercury coating was formed by deposition at -0.40 V in a solution of 5×10^{-3} mol dm^{-3} mercuric acetate + 0.1 mol dm^{-3} $HClO_4$ [23]. The size of the Hg droplet formed was calculated from the deposition charge, assuming formation of a spherical segment on the flat iridium disc [25], and also from the limiting CV current for a solution of 10^{-3} mol dm^{-3} $Ru(NH_3)_6Cl_3$ in phosphate buffer at pH 7.4 (for a hemisphere, $I_l = 2\pi nFDcr$). A radius, r_o, of ca. 4.5×10^{-6} m was calculated by each method, consistent with formation of a single hemispherical droplet.

Following deposition of the mercury droplet, the microelectrode was rinsed with distilled water and transferred to the solution to be analysed, i.e. no Hg(II) was present in the test solutions. A fresh mercury electrode surface was prepared daily and was removed at the end of each set of experiments by an oxidative linear potential scan in 1 M KSCN. This procedure prevents the formation and deposition of mercuric oxide and thus avoids the need to polish the microelectrode surface between each mercury droplet deposition [23].

2.3. Electrochemical parameters

The following conditions were used unless otherwise stated: deposition potential, -0.85 V for Cd(II), -0.80 V for Pb(II); deposition time, 180 s for Pb(II)–PDCA and Cd(II)–PDCA, and 60 s for Pb(II)–FA to minimise the possibility of ligand saturation at the electrode surface during stripping [21]. SCP: oxidising current (I_{strip}), 5×10^{-11} A, applied until the potential reached a value well past the transition plateau. DP-SV: modulation time, 0.05 s; modulation amplitude, 0.025 V; scan rate 0.010 V s^{-1}. The lower sensitivity of DC-SV precluded measurements with this mode at the microelectrode.

All data presented are raw data, i.e. no smoothing procedures were applied.

2.4. Reagents

All solutions were prepared in distilled, deionised water from an Elgastat maxima system (resistivity >18 MΩ cm). Cd(II) solutions were prepared from $Cd(NO_3)_2{\cdot}4H_2O$ (Fluka, puriss, p.a.); Pb(II) was a Metrohm ion standard solution (0.10000 ± 0.0005 mol dm^{-3}). KNO_3 solutions were prepared from solid KNO_3 (BDH, AnalaR). A stock acetate buffer solution was prepared by combining acetic acid (Prolabo, Rectapur) and sodium acetate (Janssen Chimica, pure) such that, in the final solution, each was 1 mol dm^{-3}. A stock solution of PIPES buffer (piperazine-1,4-bis(2-ethanesulfonic acid)) was prepared from the solid (Fluka, MicroSelect, $\geq 99.5\%$), and the pH adjusted to pH 6.5 with dilute carbonate-free KOH. PIPES has low surface activity on mercury [26] and low affinity for Cd(II) and Pb(II) [27]. Phosphate buffer at pH 7.4 was prepared from solid KH_2PO_4 (Fluka, puriss p.a. $>$ 99.5%) and Na_2HPO_4 (Fluka, MicroSelect, $>99.0\%$) to give a solution 0.00869 mol dm^{-3} in KH_2PO_4 and 0.0304 mol dm^{-3} in Na_2HPO_4.

$Ru(NH_3)_6Cl_3$ was from Strem Chemicals (99%), mercuric acetate was from Fluka (puriss p.a.), KSCN was from Janssen (p.a. $\geq 99\%$), and $HClO_4$ was from BDH (AnalaR). FA was the International Humic Substances Society standard Suwannee River FA (IS101F). Pyridine-2,6-dicarboxylic acid (PDCA) was from Fluka (purum).

All measurements were performed with 1.98×10^{-7} mol dm^{-3} M(II) solutions in 0.1 mol dm^{-3} KNO_3 plus 0.01 mol dm^{-3} of the appropriate buffer. Solutions were initially purged with oxygen-free nitrogen, then a nitrogen blanket was maintained during measurements. For measurements with pyridine-2,6-dicarboxylic acid, the ligand concentration was varied from ca. 10^{-5} to 10^{-4} mol dm^{-3}; with FA the total concentration ranged from ca. 14 to 55 mg dm^{-3} (equivalent to ca. 8.5×10^{-5} to 3.3×10^{-4} mol COOH groups dm^{-3} [28]). There was thus always a large excess of ligand over metal in the bulk solution. Results presented are the average of replicate experiments: for a given solution composition, at least three replicate measurements were made; for each system studied, the entire experiment was repeated at least twice (with fresh solutions and a new mercury electrode surface). Results were repeatable to within typically ca. 5%.

2.5. Degree of complex formation

2.5.1. PDCA

The protonation constants for PDCA are $\log K_1 = 4.68$, $\log \beta_2 = 6.78$ ($I = 0.1$ mol dm^{-3} $NaNO_3$, 20 °C, [29,30]). Reported stability constant values for formation of complexes with Pb(II) are scarce: $\log K_1 = 5.1$, $\log \beta_2 = 8.2$ ($I = 0.10$ mol dm^{-3} KNO_3, 25 °C [31]); $\log K_1 = 8.70$, $\log \beta_2 = 11.60$ ($I = 0.10$ M $NaNO_3$, 20 °C [29]); $\log K_1 = 8.66$, $\log \beta_2 = 11.55$ ($I = 0.50$ mol dm^{-3} $NaClO_4$, 25 °C [32]). For Cd(II) there are also few reported values: $\log K_1 = 5.7$, $\log \beta_2 = 10.0$ [31]; $\log K_1 = 6.75$, $\log \beta_2 = 11.15$ ($I = 0.10$ mol dm^{-3} $NaNO_3$, 20 °C [29]); $\log K_1 = 6.51$, $\log \beta_2 = 10.77$ ($I =$ 0.50 mol dm^{-3} $NaNO_3$, 25 °C [33]). Using the stability constant values of Anderegg [29], at pH 4.8 for the metal concentration and range of ligand concentrations employed free Pb(II) represented $\ll 1\%$ of the total Pb(II) in all cases. In the Cd(II)–PDCA system at pH 4.8 a significant proportion of the dinegatively charged CdL_2^{2-} species was formed, ranging from 12 to 59% of the total Cd(II) over the range of ligand concentrations used, with the remainder present as CdL (and free Cd(II) $\ll 1\%$ of total Cd(II) in all cases).

2.5.2. FA

Under our experimental conditions, with an excess of ligand over metal in the range ca. 90–170, the concentration of free Pb^{2+} is less than 1% of the total Pb(II) concentration [34].

3. Results and Discussion

3.1. Choice of working electrode

Due to its advantageous properties, mercury is the electrode material of choice for electroanalytical stripping measurements. In order to obtain reliable data it is essential that the surface of the working electrode is well characterised and reproducible. The classical hanging mercury drop electrode (HMDE) is clearly superior in this aspect. Despite several attempts [35,36], a true stationary micro-mercury drop in bulk form has not been fabricated to date. Thus, to obtain a mercury microelectrode surface it is necessary to plate mercury onto a micro-disk of a solid substrate. Iridium is the

best material for these purposes [37,38]: its good wettability by mercury allows formation of a perfect mercury surface (rather than the separate droplets formed on glassy carbon), and its very low solubility in mercury prevents the drawbacks of amalgam formation associated with Pt, Au, and Ag substrates.

3.2. Ligand-to-metal ratio at the electrode surface during stripping

We have shown that any possible distortion of stripping peaks due to saturation of ligand at the electrode surface during the stripping step is not a problem for SCP in the complete depletion regime [21]: the ligand-to-metal ratio at the electrode surface is maximal under these conditions, and use of the peak area will reliably quantify the accumulated metal in the unlikely event of peak splitting or broadening. In contrast, significant peak distortion may occur with DP-SV [21].

3.3. Features of SCP measurements at a microelectrode

At a macroelectrode, the stripping time regime can be varied from conditions of practically complete depletion of the electrode at very low applied oxidising currents ($I\tau_{tr}$ constant, $\tau_{tr} \propto c$; denoted as the $I\tau_{tr}$ regime), to semi-infinite linear diffusion at higher currents ($I\tau_{tr}^{1/2}$ constant, $\tau_{tr} \propto c^2$; the $I\tau_{tr}^{1/2}$ regime) [20]. The complete depletion regime offers advantages for measurements of metal ion speciation (adsorption effects are practically nonexistent and the requirement for excess ligand is minimised [21]). It is thus important to establish the experimental conditions under which the $I\tau_{tr}$ regime will hold at a microelectrode. In the complete depletion regime, the stripping curve is described simply by the Faraday and Nernst laws: $I_{strip}\tau_{tr} = c^*_{M^o} nFV_{drop}$, where τ_{tr} is the SCP transition time, $c^*_{M^o}$ is the concentration of reduced metal, M^o, in the mercury electrode, and V_{drop} is the mercury droplet volume. At a microelectrode, the applied I_{strip} should be much smaller than the steady-state limiting current (I_{SS}) so that the transition time $\tau_{tr} \gg \tau_{SS}$, where τ_{SS} is the time at which the diffusion layer thickness $\delta = r_o$. Under our experimental conditions (solution concentration, deposition time etc.) this time to achieve steady state, $\tau_{SS} = r_o^2/D$, is ca. 0.02 s, and the corresponding I_{SS} is 6×10^{-9} A. For practical purposes we recommend that I_{strip} is ca. 100 × less than I_{SS}. We have chosen an I_{strip} of 5×10^{-11} A for our measurements (corresponding to τ_{tr} values > 1 s).

Measurement of the stripping time for Pb(II) as a function of the applied stripping current at a microelectrode illustrates that practically achievable conditions always correspond to the $I\tau_{tr}$ regime (Fig. 1). This observation is consistent with the expected thin-film behaviour associated with the very small mercury electrode volume in this case.

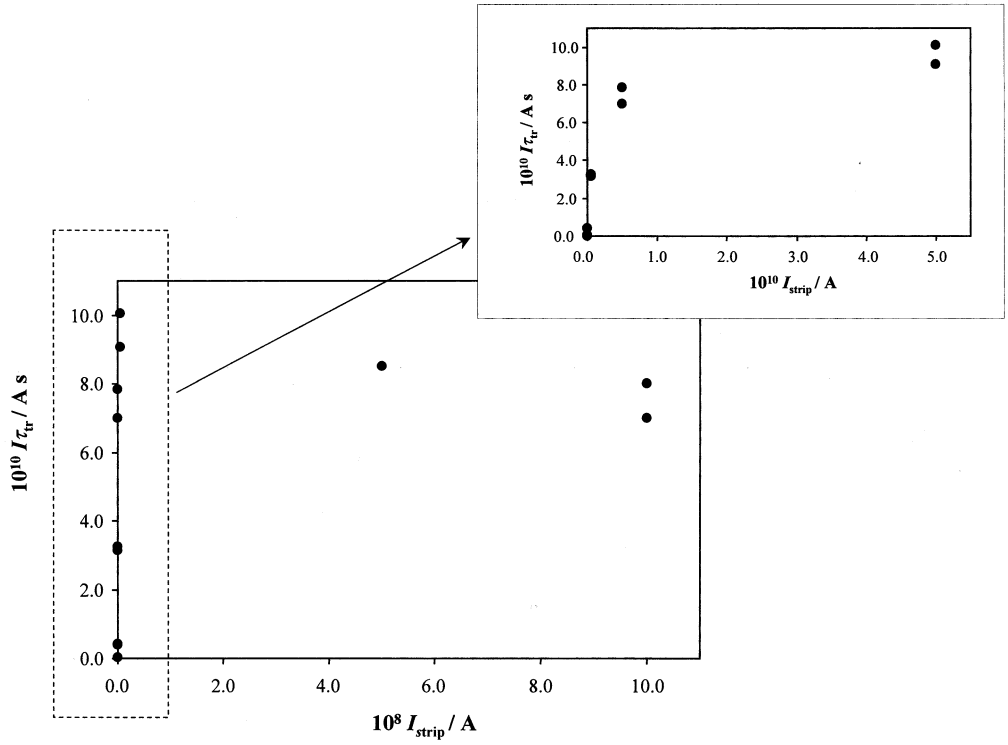

Fig. 1. Magnitude of SCP transition time, τ_{tr}, as a function of applied oxidising current, I_{strip}. [Pb(II)] = 1.98×10^{-7} mol dm^{-3}, $t_d = 600$ s, $E_d = -0.90$ V.

The lowest stripping current density that could be practically used at the microelectrode in deoxygenated solution (0.39 A m^{-2}: $I = 5 \times 10^{-11}$ A for area 1.3×10^{-10} m^2) was ca. 100 × greater than that at a macro HMDE (3.8×10^{-3} A m^{-2}: $I = 2 \times 10^{-9}$ A for area 5.2×10^{-7} m^2 [20]) reflecting the greater flux of oxygen, or other trace oxidants, to the microelectrode surface under radial diffusion conditions. With a semi-microelectrode (1×10^{-4} m diameter gold wire), it was claimed that deoxygenation of the sample is not necessary prior to SCP measurements [39,40]. However, we have found that removal of oxygen is required for reliable SCP measurements of trace metal concentrations at a true microelectrode. During stripping, the flux of dissolved oxygen will add to the effective oxidising 'current', thus reducing the magnitude of the stripping signal in a manner which may not be well controlled. No signal was detectable under our measurement conditions in a fully oxygenated solution. This observation is a consequence of the requirement for application of a small stripping current in order to maintain $\tau_{tr} \gg \tau_{SS}$ (see above). Note that the practical necessity for removal of oxygen also depends on the chosen deposition potential (i.e. the position with respect to the oxygen wave), and on the nature of the electrode surface (with respect to the irreversibility of oxygen reduction). Oxygen removal procedures have also been shown to be necessary for in situ SW-SV measurements of trace metals [41].

3.4. Lability criterion at a microelectrode

Microelectrode surfaces have dimensions smaller than the thickness of the operational diffusion layer. In this situation the diffusion regime in the diffusion layer is radial. This feature means that the relative contributions of diffusional and kinetic fluxes to the overall mass transport to a microelectrode surface, and thus the ensuing lability of metal complex species, may be very different from that in effect at a macroelectrode. In fact the lability of metal complex species will tend to be reduced at a microelectrode, due to enhanced diffusion. Galceran et al. [19] presented a rigorous analytical derivation of the following lability criterion for a microelectrode, valid for ligand excess (pseudo first order kinetics) and steady state conditions:

$$\frac{k_d^{1/2} K^{-1/2} r_o D_M^{1/2}}{D_{ML} c_L^{*1/2}} > 1 \quad (1)$$

where k_d is the complex dissociation rate constant (related to the equilibrium stability constant for ML, K, and the association rate constant, k_a, through $K = k_a/k_d$), D_M and D_{ML} are the diffusion coefficient of the free metal ion and that of the metal complex respectively, and c_L^* is the concentration of ligand in the bulk solution.

This criterion was calculated for the various systems studied in the present work and results are given in the following sections. In aqueous systems, the overall complex formation rate constant, k_a, is defined by [42] (i) the rate constant for water substitution in the inner coordination sphere of the metal ion, k_{-w} (for Pb(II) k_{-w} is 7×10^9 s^{-1} [43], and for Cd(II) is 3×10^8 s^{-1} [44]), and (ii) the stability constant for the intermediate outer sphere complex that is typically estimated on the basis of electrostatics [43]. For Pb(II) this gives an overall k_a of 10^{10} M s^{-1} and for Cd(II), 10^9 M s^{-1} [45]. $D_{Pb} = 8.3 \times 10^{-10}$ m^2 s^{-1} and $D_{Cd} = 7.0 \times 10^{-10}$ m^2 s^{-1} [46].

3.5. Adsorption effects

The general adsorption characteristics of PDCA [47] and FA [48] have been discussed in the literature and are summarised in our previous work [21]. We have shown, using a conventional HMDE, that SCP in the complete depletion ($I\tau_{tr}$) regime is basically unaffected by adsorption of ligand and induced adsorption of the metal ion [21]. In contrast, the significant signal enhancements observed for SCP in the semi-infinite linear diffusion regime and for DC-SV and DP-SV could be explained by consideration of the characteristic time constants for adsorption of ligand at a macroelectrode (via pure diffusion and convective diffusion) [21].

At a microelectrode, the characteristic time constant, τ, for adsorption of ligand, L, in the linear adsorption regime is given by $r_o K_{H_L}/D_L$ for steady-state diffusion (where K_{H_L} is the Henry coefficient for adsorption of L, and where the initial transient part for $t < \tau_{SS}$ has been ignored). Thus, relative to the case of convective diffusion at a macroelectrode [21], the adsorption process is more rapid and τ is reduced by a factor of approximately 100 to ca. 0.05 s for an electrode of the size used in this work ($r_o = 4.5 \times 10^{-6}$ m) and not too strong adsorption (K_{H_L} ca. 10^{-5} m). This implies that during the stripping step at a microelectrode the surface excess of L, Γ_L, will be close to its equilibrium value even with transient techniques such as DP-SV (pre-pulse period typically ca. 1s). The concentration and time dependence of adsorption processes at a microelectrode are therefore likely to be reduced relative to the macroelectrode case.

With transient-type techniques such as DP-SV at a microelectrode, interpretation of measurements of metal speciation can become even more complicated than at a HMDE. This arises because, in addition to possible reduction in the signal due to the lower lability of metal complex species under radial diffusion conditions (a feature common to all stripping techniques), adsorption processes may cause concomitant disproportional signal enhancement.

Table 1
Effect of PDCA on the magnitude of Cd(II) stripping signals at pH 4.8

$10^5\ c^*_{PDCA}$/mol dm^{-3}	(Peak magnitude in presence of PDCA)/(peak magnitude for Cd(II)) [a]		
	SCP		DP-SV
	Peak height	Peak area	Peak height
1.02	0.53	0.54	0.32
2.03	0.47	0.50	0.38
4.06	0.34	0.36	0.39
9.08	0.25	0.31	0.30

[a] $[Cd(II)] = 1.98 \times 10^{-7}$ mol dm^{-3}, $t_d = 180$ s, $E_d = -0.90$ V.

3.6. The system Cd(II)–PDCA, pH 4.8

PDCA itself is not adsorbed at this pH and the neutral Cd(II)–PDCA complex is not expected to be significantly adsorbed over the potential range of Cd(II) oxidation (in addition, there is a significant proportion of CdL_2^{2-} present, see above). At a HMDE, no change in the magnitude of Cd(II) SCP or SV signals was observed on addition of PDCA [21], consistent with a fully labile system free from adsorption interferences.

The ratio of Cd(II) peak signals in the presence of a range of PDCA concentrations relative to that for free Cd(II) recorded at a microelectrode is given in Table 1, and the corresponding experimental stripping curves are shown in Fig. 2.

The values reported in Table 1 show that the reduction in SCP peak area and DP-SV peak height are the same at the highest concentration of PDCA. Such a result is expected for this system which is not influenced by adsorption [21]. At lower ligand concentrations, the greater apparent decrease in the DP-SV signal is probably due to the effect of ligand saturation at the electrode surface on the peak shape. Fig. 2(b) shows that the DP-SV peaks are broadened and distorted at 1.02×10^{-5} mol dm^{-3} PDCA, become sharper (and higher) as the concentration increases to 2.03 and 4.06×10^{-5} mol dm^{-3}, then the height decreases at higher ligand concentration due to the ensuing reduction in lability.

From application of Eq. (1), taking $D_{ML} = D_M$ [47], and using the stability constants of Anderegg [29], the lability parameter under our conditions is calculated to be 0.3 for $c^*_{PDCA} = 10^{-5}$ mol dm^{-3} and 0.1 for $c^*_{PDCA} = 10^{-4}$ mol dm^{-3} The decrease in the Cd(II) signal in the presence of PDCA reported in Table 1 thus seems to reflect the predicted reduced lability of Cd(II)–PDCA complexes at a microelectrode. In the range of ligand concentrations studied, this system is an intermediate stage with respect to lability (lability criterion as defined by Eq. (1) is close to unity) and the SCP

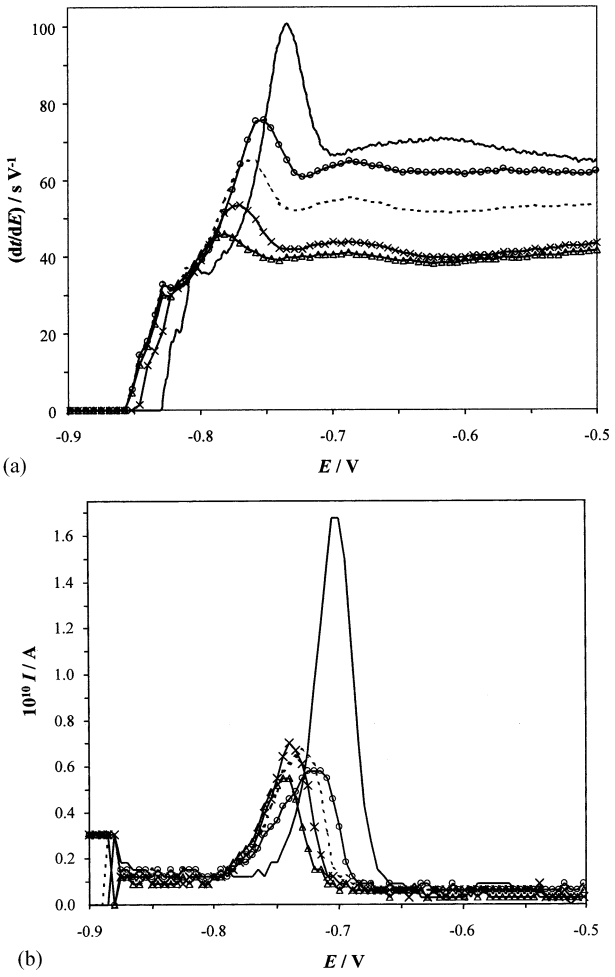

Fig. 2. Stripping curves for Cd(II) in the presence of increasing concentration of PDCA at pH 4.8. (a) SCP, (b) DP-SV. $t_d = 180$ s, SCP $I_{strip} = 5 \times 10^{-11}$ A. $[Cd(II)] = 1.98 \times 10^{-7}$ mol dm^{-3}. 10^5[PDCA]/mol dm^{-3} = 0 (—); 1.02 (–○–); 2.03 (---); 4.06 (– × –); 9.08 (–△–).

results are sensitive to this situation. The decrease in the SCP stripping peaks as the ligand concentration is increased (Fig. 2(a)) thus reflects the decreasing lability. Another factor to be considered in this system is the formation of an increasing proportion of CdL_2^{2-} species as the concentration of PDCA is increased (Section 2.5.1). Although measurements at a HMDE suggested that $D_{CdL_2} \approx D_{Cd}$ [21], it is possible that the CdL_2^{2-} species has a slightly lower D value than CdL or free Cd(II). The radial diffusion conditions at a microelectrode result in larger fluxes towards the electrode surface, as compared to the macroelectrode case, and this situation may be more sensitive to small differences in D values. Anyway, the more stable CdL_2^{2-} species may be expected to be less labile than CdL at a microelectrode.

Table 2
Effect of PDCA on the magnitude of Pb(II) stripping signals at pH 4.8

$10^5\ c^*_{PDCA}$/mol dm^{-3}	(Peak magnitude in presence of PDCA)/(peak magnitude Pb(II)) [a]		
	SCP		DP-SV
	Peak height	Peak area	Peak height
1.02	0.51	0.59	0.11
2.03	0.48	0.53	0.15
4.06	0.41	0.45	0.21
9.08	0.47	0.48	0.34

[a] $[Pb(II)] = 1.98 \times 10^{-7}$ mol dm^{-3}, $t_d = 180$ s, $E_d = -0.90$ V.

3.7. The system Pb(II)–PDCA, pH 4.8

The neutral 1:1 Pb(II)–PDCA complex will adsorb on the electrode surface in the potential range over which Pb is being stripped from the electrode (close to the pzc). The adsorption properties of Pb(II)–PDCA are assumed to be comparable to those of the diprotonated ligand, H_2L [21]. The ratio of Pb(II) peak signal in the presence of a range of PDCA concentrations relative to that for free Pb(II) is given in Table 2. The corresponding experimental curves shown in Fig. 3 indicate that DP-SV is again affected by saturation of ligand at the electrode surface during stripping. The increase in the relative DP-SV signal as the concentration of PDCA is increased probably reflects a combination of enhancement due to induced adsorption [21] and the effect of saturation of the ligand at the electrode surface during stripping on the shape of the curves (Fig. 3(b)).

The lability of the Pb(II)–PDCA at the microelectrode was calculated from Eq. (1). Taking $D_{ML} = D_M$ [47], and using the stability constants of Anderegg [29], the lability criterion is calculated to be 0.01 for $c^*_L = 10^{-5}$ mol dm^{-3} and 0.003 for $c^*_L = 10^{-4}$ mol dm^{-3}. Using a stability constant of $10^{8.1}$ calculated from our previous work [21], the lability criterion is 0.04 and 0.01, respectively. Given the uncertainties in K and k_a values, the lability criterion must be taken as an order of magnitude estimation of the expected behaviour of a given system. For Pb(II), the lability criterion is significantly less than 1.0 for all ligand concentrations considered, and the normalised magnitude of the Pb(II) SCP stripping peak in the presence of ligand was insensitive to the concentration of ligand (Table 2).

Comparison of the relative magnitudes of the lability criterion for Pb(II)–PDCA and Cd(II)–PDCA shows that we might expect the Pb(II) complexes to be the less labile. In practice the PDCA complexes with Pb(II) and Cd(II) were of similar lability at the lowest ligand concentration, and the Cd(II) complexes became increasingly less labile as the PDCA concentration increased (Tables 1 and 2). These observations probably reflect a combination of (i) uncertainties in calculation of the lability criterion (i.e. uncertainties in K and k_a), and (ii) the contribution from CdL_2^{2-} species (Section 3.6). It must be realised that the lability observed for a given system is a combination of the interplay between complex stability (K) and the overall complex formation rate constant (k_a). For example, in the case of FAs, it has been demonstrated that Pb(II) and Cd(II) complexes have comparable labilities because the influence of the greater thermodynamic stability of the Pb(II) complexes is offset by the substantially higher k_a value for this metal ion (Section 3.4) [45].

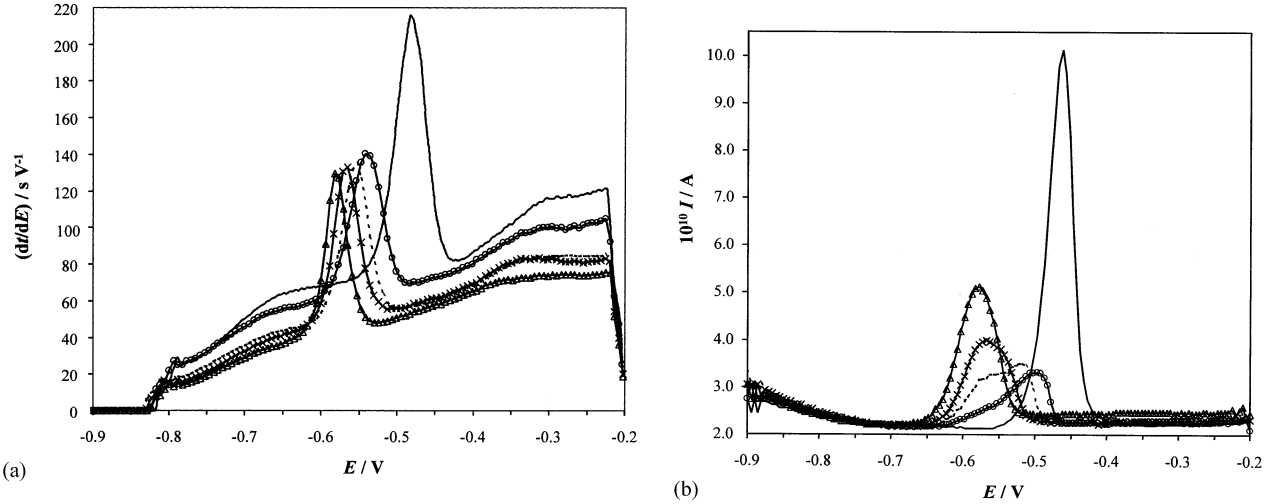

Fig. 3. Stripping curves for Pb(II) in the presence of increasing concentration of PDCA at pH 4.8. (a) SCP, (b) DP-SV. $t_d = 180$ s, SCP = I_{strip} 5×10^{-11} A. $[Pb(II)] = 1.98 \times 10^{-7}$ mol dm^{-3}. 10^5[PDCA]/mol dm^{-3} = 0 (—); 1.02 (–○–); 2.03 (---); 4.06 (– × –); 9.08 (–△–).

Table 3
Effect of FA on the magnitude of Pb(II) stripping signals at pH 6.5

c^*_{FA}/mg dm^{-3}	10^5 c^*_L/mol dm^{-3} [a]	(Peak magnitude in presence of FA)/(peak magnitude Pb(II)) [b]		
		SCP		DP-SV
		Peak height	Peak area	Peak height
14.0	8.5	0.64	0.75	0.88
27.5	17.0	0.52	0.61	0.72
54.5	33.0	0.35	0.41	0.62

[a] Equivalent to the total number of carboxyl groups in Suwannee River FA (6.1 mmol g^{-1} [28]).
[b] [Pb(II)] = 1.98×10^{-7} mol dm^{-3}, $t_d = 60$ s, $E_d = -0.80$ V.

3.8. The system Pb(II)–FA, pH 6.5

Metal complexes with FAs are representative of those present in natural waters. These heterogeneous macromolecular ligands are important complexants for metal ions, and may play a crucial role in metal ion buffering, and thus in maintenance of life in aquatic systems [49]. A reliable, artefact-free method for studying the complexation properties of such ligands is thus a crucial first step towards a rational methodology for in situ monitoring of metal ion speciation. Metal complexes with macromolecular ligands will have reduced diffusion coefficients as compared to that for the free metal ion, thus, even if such complexes are labile, some reduction in stripping signal is expected relative to that for an equivalent concentration of free metal ions.

The lability of Pb(II)–FA at the microelectrode was predicted from Eq. (1). Taking the diffusion coefficient reported for free FA (ca. 3×10^{-10} m^2 s^{-1} [50]) as a reasonable estimate for D_{ML}, estimating c^*_L as being equivalent to the concentration of carboxyl groups (Section 2.4), and a log K value of 5 (determined for an aquatic FA under conditions (pH and metal ion loading) comparable to those used herein [51]), the lability criterion is calculated to be 47 for a FA concentration of 14 mg dm^{-3}, and 24 for 54.5 mg dm^{-3}. Thus complexes formed in this system are expected to be still labile at the microelectrode.

The change in peak magnitude in the presence of FA, relative to that for free Pb(II) is given for each technique in Table 3, and the corresponding experimental curves are shown in Fig. 4.

The SCP peaks are broadened in the presence of FA, as is shown by the greater decrease in peak height as compared to peak area (Table 3). Peak broadening may arise from saturation of ligand at the electrode surface during stripping and/or may be the consequence of heterogeneity, i.e. it reflects the formation of a range of Pb(II)–FA complexes of slightly different stability. Experimental conditions were chosen to minimise the possibility of ligand saturation during stripping (short deposition time and relatively large excess of ligand in the bulk solution) and SCP has a lower requirement for excess ligand than do the transient SV techniques [21]. It is thus likely that the observed peak broadening is at least in part due to the influence of ligand heterogeneity. As discussed in more detail in our previous work [21], an advantage of SCP (under conditions approaching complete depletion) is that the peak area provides correct quantitation of systems in which peak broadening has occurred (by whatever process).

The relative decrease in the DP-SV peaks is less than that for SCP for all concentrations of FA studied. This implies that in this system the effect of adsorption-induced enhancement of the pulse voltammetric signals dominates over any reduction in peak height due to saturation of ligand at the electrode surface (c.f. results for Pb(II)–PDCA, Section 3.7). Although adsorption processes are more rapid at a microelectrode (Section 3.5), in the case of heterogeneous ligands, Γ_L may well not be at its equilibrium value in transient techniques.

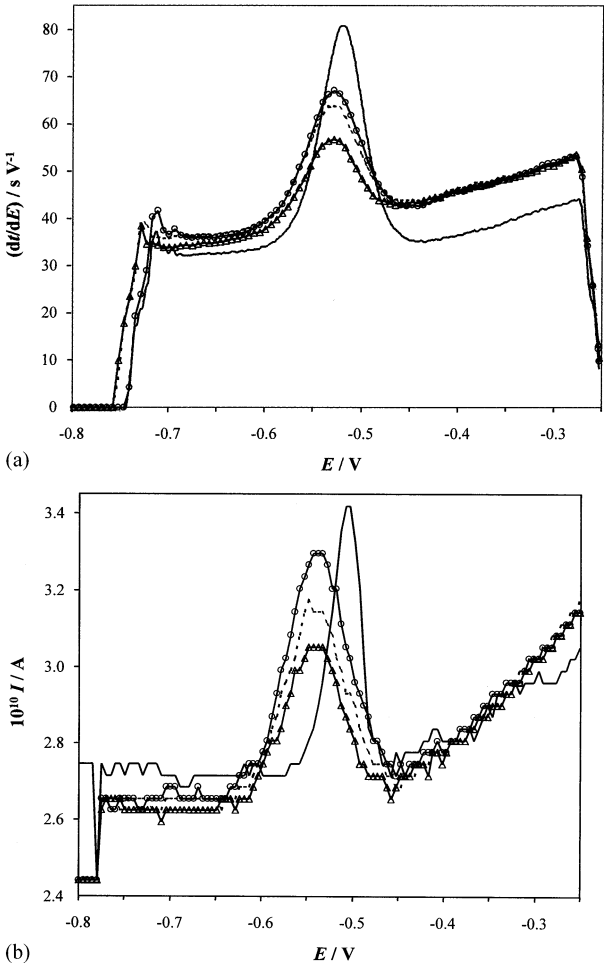

Fig. 4. Stripping curves for Pb(II) in the presence of increasing concentration of FA at pH 6.5. (a) SCP, (b) DP-SV. $t_d = 60$ s, SCP $I_{strip} = 5 \times 10^{-11}$ A. [Pb(II)] = 1.98×10^{-7} mol dm^{-3}. [FA]/mg dm^{-3} = 0 (—);13.7 (–○–); 27.3 (---); 54.1 (–△–).

The adsorption of FA onto mercury is dependent on potential, time and pH [48,52–55]. A consequence of the heterogeneity of FA is that K_{H_L} for this ligand is represented by a distribution of values, and thus the resulting τ for adsorption of L will correspond to some average of an underlying distribution. Since Pb oxidation occurs at a potential close to the pzc (at which adsorption of FA is maximal [52]), these factors will almost certainly play a significant role in determining the overall impact of adsorption on the stripping signal. Under such conditions it is practically unrealistic to reconstruct Γ_L as a function of t (or potential). This is particularly true for SV at a microelectrode: in this case any adsorption effects are overlaid with those of a possible decrease in signal due to reduced lability (affecting the accumulation) together with probable saturation of ligand at the electrode surface during the reoxidation process.

For labile complexes, for the case of nonequal diffusion coefficients for the free metal and complex species, under conditions of complete complex formation (i.e. $c^*_{Pb_{free}} \ll c^*_{Pb_{total}}$, as expected under our conditions, Section 2.5.2): $I^L_p/I_p = D_{ML}/D_M$ on microelectrodes [11], where D_M and D_{ML} are the diffusion coefficients for the free and complexed metal ion respectively, I_p is the peak current (DP-SV) or peak (dt/dE) value (SCP), and superscript L denotes in the presence of ligand. Assuming that SCP under conditions of complete depletion gives a reliable measure of the signal unaffected by adsorption [21], then the expected reduction in peak area due to the reduced diffusion coefficient for the metal species on addition of FA to a solution of Pb(II) (taking $D_{ML} = 3 \times 10^{-10}$ m^2 s^{-1}) is calculated to be 0.36, which is in good agreement with the experimentally observed value of 0.41 at a FA concentration of 54.5 mg dm^{-3} (Table 3).

4. Conclusions

The lability of metal complex species has been predicted to be reduced at a microelectrode, due to enhanced diffusion [19]. This effect influences the accumulation step which is identical for all stripping techniques, including SCP and SV. SCP experiments at a microelectrode are essentially of a steady-state nature and correspond to complete depletion. SCP data are consistent with the theoretical lability predictions and are not influenced by adsorption processes.

Adsorption processes will be faster at a microelectrode, as compared to a macroelectrode, but for short timescale techniques such as DP-SV adsorption may still be in a transient stage for the case of heterogeneous macromolecular ligands such as FAs. This situation is reflected in adsorption-induced enhancement of the stripping signals which cannot be analysed in a straightforward manner.

Saturation of ligand at the surface of the electrode during stripping causes severe peak distortion in DP-SV, but has no detrimental impact on SCP measurements. This is due to the much lower requirement for excess ligand in SCP and to the fact that use of peak area accounts for any peak distortion. In situ testing of SCP in conjunction with microelectrodes for measurement of metal ion speciation merits further attention.

5. List of symbols and abbreviations

c^*_L	bulk ligand concentration (mol dm^{-3})
δ	diffusion layer thickness (m)
D	diffusion coefficient (m^2 s^{-1})
E_d	deposition potential (V)
k_a	association rate constant
k_d	dissociation rate constant
K_H	Henry adsorption coefficient (m)
I_{strip}	applied stripping (oxidising) current (A)
K	equilibrium stability constant for formation of ML
μ	reaction layer thickness (m)
ML	metal–ligand complex
r_o	electrode radius (m)
t	time (s)
t_d	deposition time (s)
τ_{tr}	SCP transition time (s)

Acronyms

CV	cyclic voltammetry
DC	direct current
DP	differential pulse
FA	fulvic acid
HMDE	hanging mercury drop electrode
PDCA	pyridine-2,6-dicarboxylic acid
pzc	potential of zero charge
SCP	stripping chronopotentiometry
SS	steady state
SV	stripping voltammetry
SW	square wave

Acknowledgements

This study was facilitated by financial support from the Nederlandse Organisatie voor Wetenschappelijk Onderzoek and The British Council under the UK–Netherlands partnership program in science (project no. PPS686). A grant from The Royal Society of Chemistry Research Fund towards purchase of the microelectrodes and polishing system is acknowledged. This

work was performed in the context of the EU Framework 5 project BIOSPEC (EVK1-CT-2001-00086).

References

[1] H.P. van Leeuwen, in: J. Buffle, G. Horvai (Eds.), In Situ Monitoring of Aquatic Systems. Chemical Analysis and Speciation, Wiley, Chichester, 2000, p. 253.
[2] K. Simkiss, M.G. Taylor, J. Environ. Monit. 3 (2001) 15.
[3] E. Wasserman, A.R. Felmy, A. Chilakapati, Coll. Surf. B 18 (2000) 19.
[4] R.J.M. Hudson, Sci. Tot. Environ. 219 (1998) 95.
[5] W.G. Sunda, S.A. Huntsman, Sci. Tot. Environ. 219 (1998) 165.
[6] J. Buffle, W. Stumm, in: J. Buffle, R.R. De Vitre (Eds.), Chemical and Biological Regulation of Aquatic Systems, Lewis, Boca Raton, 1994, p. 1.
[7] H.P. van Leeuwen, H.G. De Jong, K. Holub, J. Electroanal. Chem. 260 (1989) 213.
[8] H.P. van Leeuwen, R.F.M.J. Cleven, J. Buffle, Pure Appl. Chem. 61 (1989) 255.
[9] H.P. van Leeuwen, J. Buffle, J. Electroanal. Chem. 296 (1990) 359.
[10] J. Galceran, J. Salvador, J. Puy, F. Mas, H.P. van Leeuwen, J. Electroanal. Chem. 391 (1995) 29.
[11] J. Buffle, M.-L. Tercier-Waeber, in: J. Buffle, G. Horvai (Eds.), In Situ Monitoring of Aquatic Systems. Chemical Analysis and Speciation, Wiley, Chichester, 2000, p. 279.
[12] S. Daniele, M.-A. Baldo, P. Ugo, G.-A. Mazzocchin, Anal. Chim. Acta 219 (1989) 9.
[13] S. Daniele, M.-A. Baldo, P. Ugo, G.-A. Mazzocchin, Anal. Chim. Acta 219 (1989) 19.
[14] J.S. Feinberg, W.J. Bowyer, Microchem. J. 47 (1993) 72.
[15] M.-L. Tercier, J. Buffle, Anal. Chem. 68 (1996) 3670.
[16] S. Daniele, C. Bragato, M.A. Baldo, J. Wang, J. Lu, Analyst 125 (2000) 731.
[17] J.P. Pinheiro, H.P. van Leeuwen, Environ. Sci. Technol. 35 (2001) 894.
[18] H.P. van Leeuwen, J.P. Pinheiro, J. Electroanal. Chem. 471 (1999) 55.
[19] J. Galceran, J. Puy, J. Salvador, J. Cecília, H.P. van Leeuwen, J. Electroanal. Chem. 505 (2001) 85.
[20] R.M. Town, H.P. van Leeuwen, J. Electroanal. Chem. 509 (2001) 58.
[21] R.M. Town, H.P. van Leeuwen, J. Electroanal. Chem. 523 (2002) 1.
[22] F.C. Anson, J.B. Flanagan, K. Takahashi, A. Yamada, J. Electroanal. Chem. 67 (1976) 253.
[23] M.-L. Tercier, N. Parthasarathy, J. Buffle, Electroanalysis 7 (1995) 55.
[24] R.M. Wightman, D.O. Wipf, in: A.J. Bard (Ed.), Electroanalytical Chemistry, vol. 15, Marcel Dekker, New York, 1987, p. 267.
[25] M. Corbetta, M.A. Baldo, S. Daniele, G.A. Mazzocchin, Ann. Chim. 86 (1996) 77.
[26] M.T.S.D. Vasconcelos, M.A.G.O. Azenha, C.M.R. Almeida, Anal. Biochem. 265 (1998) 193.
[27] H.M.V.M. Soares, P.C.F.L. Conde, Anal. Chim. Acta 421 (2000) 103.
[28] E.C. Bowles, R.C. Antweiler, P. MacCarthy, in: R.C. Averett, J.A. Leenheer, D.M. McKnight, K.A. Thorn (Eds.), Humic Substances in the Suwannee River, Georgia: Interactions, Properties, and Proposed Structures, US Geological Survey Water-Supply Paper 2373, United States Government Printing Office, 1994, p. 115.
[29] G. Anderegg, Helv. Chim. Acta 43 (1960) 414.
[30] C. Timberlake, J. Chem. Soc. (1964) 1229.
[31] K. Suzuki, K. Yamasaki, Naturwissenschaft 44 (1957) 396.
[32] L. Campanella, G. de Angelis, A. Napoli, Bull. Soc. Chim. Belges 81 (1972) 489.
[33] R. Scharff, M. Paris, Bull. Soc. Chim. Fr. (1968) 3184.
[34] J. Buffle, F.-L. Greter, J. Electroanal. Chem. 101 (1979) 231.
[35] L. Novotný, M. Heyrovský, Trends Anal. Chem. 6 (1987) 176.
[36] R.M. Town, M.-L. Tercier, N. Parthasarathy, F. Bujard, S. Rodak, C. Bernard, J. Buffle, Anal. Chim. Acta 302 (1995) 1.
[37] S.P. Kounaves, J. Buffle, J. Electrochem. Soc. 133 (1986) 2495.
[38] S.P. Kounaves, J. Buffle, J. Electroanal. Chem. 216 (1987) 53.
[39] J. Wang, D. Larson, N. Foster, S. Armalis, J. Lu, X. Rongrong, K. Olsen, A. Zirino, Anal. Chem. 67 (1995) 1481.
[40] J. Wang, N. Foster, S. Armalis, D. Larson, A. Zirino, K. Olsen, Anal. Chim. Acta 310 (1995) 223.
[41] M.-L. Tercier-Waeber, J. Buffle, Environ. Sci. Technol. 34 (2000) 4018.
[42] H.P. van Leeuwen, J. Radioanal. Nucl. Chem. 246 (2000) 487.
[43] F.M.M. Morel, J.G. Hering, Principles and Applications of Aquatic Chemistry, Wiley, New York, 1993, p. 400.
[44] M. Eigen, Pure Appl. Chem. 6 (1963) 97.
[45] J.P. Pinheiro, A.M. Mota, H.P. van Leeuwen, Coll. Surf. A 151 (1999) 181.
[46] M.O. von Stackelberg, M. Pilgram, V. Toome, Z. Elektrochem. 57 (1953) 342.
[47] J. Buffle, A.M. Mota, M.L.S. Simões Gonçalves, J. Electroanal. Chem. 223 (1987) 235.
[48] J. Buffle, A. Cominoli, J. Electroanal. Chem. 121 (1981) 273.
[49] J. Buffle, Complexation Reactions in Aquatic Systems. An Analytical Approach, Ellis Horwood, Chichester, 1988.
[50] G.R. Aiken, P.A. Brown, T.I. Noyes, D.J. Pinckney, in: R.C. Averett, J.A. Leenheer, D.M. McKnight, K.A. Thorn (Eds.), Humic Substances in the Suwannee River, Georgia: Interactions, Properties, and Proposed Structures, US Geological Survey Water-Supply Paper 2373, US Government Printing Office, 1994, p. 89.
[51] J. Buffle, J.J. Vuilleumier, M.L. Tercier, N. Parthasarathy, Sci. Total Environ. 60 (1987) 75.
[52] J. Buffle, A. Cominoli, J. Electroanal. Chem. 121 (1981) 273.
[53] B. Raspor, P. Valenta, Mar. Chem. 25 (1988) 211.
[54] J.P. Pinheiro, A.M. Mota, M.S. Gonçalves, H.P. van Leeuwen, Environ. Sci. Technol. 28 (1994) 2112.
[55] M. Ochs, B. Ćosović, W. Stumm, Geochim. Cosmochim. Acta 58 (1994) 639.